CHINA FOUNDRY Research & Development
Vol. 23 No. 1 January 2026
www.springer.com/41230
https://doi.org/10.1007/s41230-025-3152-z

# Influence of ultrasonic agitation on dispersion of fibers in a shell mold for investment casting

**Zhi-cheng Feng[1], *Kai Lü[1, 2, 3], Yan Lu[1], Wen-bo Jin[1], and Lei Che[1]**

*1. School of Materials Science and Engineering, Inner Mongolia University of Technology, Hohhot 010051, China*

*2. Engineering Research Center of Development and Processing Protection of Advanced Light Metals, Ministry of Education, Hohhot 010051, China*

*3. The Inner Mongolia Advanced Materials Engineering Technology Research Center, Hohhot 010051, China*



**Abstract:** To develop a suitable production process for fiber reinforced investment casting shell mold, three methods were studied: the traditional method ($M_1$), the method of adding fiber into silica sol with mechanical stirring and ultrasonic agitation ($M_2$), and the method of adding fiber into slurry with mechanical stirring and ultrasonic agitation for durations of 3, 15, 30, and 45 min ($M_3$). The bending strength, high-temperature self-load deformation, and thermal conductivity of the shell molds were investigated. The results reveal that the enhancement of fiber dispersion through ultrasonic agitation improves the comprehensive performance of the shell molds. The maximum green bending strength of the shell mold by $M_2$ reaches 3.29 MPa, which is 29% higher than that of the shell mold prepared by $M_1$. Moreover, the high-temperature self-load deformation of the shell mold is reduced from 0.62% to 0.44%. In addition, simultaneous ultrasonic agitation and mechanical stirring effectively shorten the slurry preparation time while maintaining comparable levels of fiber dispersion. With the process $M_3$-45 min, the fillers are uniformly dispersed in the slurry, and the fired bending strength and the high-temperature self-load deformation reach 6.25 MPa and 0.41%, respectively. Therefore, the proposed ultrasonic agitation route is promising for the fabrication of fiber-reinforced shell molds with excellent fibers dispersion.

**Keywords:** investment casting; steel fibers; fiber-reinforced shell; ultrasonic agitation; thermal conductivity

**CLC numbers:** TG221 **Document code:** A **Article ID:** 1672-6421(2026)01-108-09

## 1 Introduction

Investment casting enables to produce complex geometries with near-net shape and high precision[1, 2], showing promise in aerospace and other manufacturing areas[3, 4]. However, the low green bending strength of silica sol shell limits their application in production of castings[5, 6]. Hence, the shell thickness is usually increased to improve the bending strength, which is attained at the expense of residual strength and shell permeability[7]. A thicker shell also decreases the cooling rate of the casting and leads to the grain coarsening, which is compromising the mechanical properties of as-cast products[8, 9].

Fiber-reinforced shells offer an innovative approach for the preparation of investment casting shell molds. By incorporating fibers as reinforcing agents, it is possible to significantly reduce both the thickness and preparation time of the shell molds. The incorporation of organic fibers can enhance the air permeability of the shell molds[10, 11], allowing for more effective gas release during casting, which can improve the quality of the cast parts. Furthermore, the inclusion of inorganic fibers can improve the high-temperature performance of the shell molds[12, 13], enabling them to withstand the thermal stress encountered during the casting process. In addition, the properties of the shell molds can be tailored through the use of fiber hybrids[14]. Lu et al.[15] have demonstrated that the addition of carbon fibers to silica sol can increase the thermal conductivity of the shell molds. But, the organic fibers are burnt out at high temperatures which makes its reinforcement effect is limited. Thus, steel fibers are incorporated as a reinforcing phase due to their high resistance to elevated temperatures. However, irregular grooves on the surface of steel fibers hinder the proper wetting and increases the surface friction of steel fibers. This leads to steel fibers being easily intertwined, and this phenomenon becomes more prominent with increasing

***Kai Lü**

Male, born in 1983, Ph. D., Professor. Research interest: investment casting.

E-mail: nmglk83@imut.edu.cn

**Received: 2023-11-15; Revised: 2024-02-11; Accepted: 2024-07-15**

fiber content. The intertwined fibers weaken the performance of fiber-reinforced shell molds and can even act as the crack sources[16]. In the traditional slurry preparation, the shear force generated by mechanical stirring is used to disperse the filler[17] and fiber[13]. However, for steel fibers, it is difficult to disperse completely by mechanical stirring. Therefore, it is necessary to find a way to combine or replace mechanical stirring to improve steel fiber dispersion during the preparation of fiber-reinforced shell molds. Wang et al.[18] have indicated that the fibers can be dispersed using the cavitation and microjet effects, which are produced by ultrasonic waves. The addition of hydroxypropyl methylcellulose (HPMC) also increases the mutual repulsion between fibers and improves fiber dispersion[19]. The surface of fibers can also be modified by silane coupling agent to improve the dispersion of fibers[20]. Ultrasonic agitation is indeed a simple and efficient method for dispersing steel fibers in a matrix.

In this study, to establish the optimal preparation conditions for fiber-reinforced shell molds, three different dispersion methods are designed: the traditional method ($M_1$), the method of adding fiber into silica sol with mechanical stirring and ultrasonic agitation ($M_2$), and the method of adding fiber into slurry with mechanical stirring and ultrasonic agitation for varius durations. Meanwhile, as the ultrasonication affects the filler, it is also expected to shorten the time required for slurry preparation.

# 2 Materials and methods

## 2.1 Shell preparation

316L steel fibers with a length of 4 mm and diameters of 10±1 μm were used as the reinforcement material. Figure 1 shows the detailed morphology of a single steel fiber. It possesses a cylindrical shape and has a rough surface with grooves. The fibers were only added to the back and sealing layers of the shell to avoid the influence of steel fibers on the surface roughness of the primary layer. The fiber content was 0.15% of the filler weight. The raw materials for preparation of investment casting shell slurry are described in Table 1, where silica sol was from Linyi Kehan Silicon Products Co., Ltd., China, zircon sand and mullite sand were from Zhengzhou Honghu Chemical Co., Ltd., China. An electric mixer (Hebei Shengxing Instrument Equipment Co., Ltd., China) was used for mechanical stirring.

Three different methods were designed during the preparation of slurry. As shown in Fig. 2(a), the traditional method ($M_1$) involves of adding fibers to the slurry with a binder-to-filler ratio of 1:1.4 and mechanically stirring the mixture for 2 h to prepare the desired slurry. In second method ($M_2$), the fibers are added to the silica sol and subject to ultrasonic agitation and mechanical agitation for 3 min, as shown in Fig. 2(b). Combined with mechanical stirring, the fibers are completely dispersed in the silica sol. Then, the filler is added and stirred for 2 h to prepare the desired slurry. The third method ($M_3$) is proposed in Fig. 2(c). The fibers are added in the slurry, then stirred by both mechanical stirring and ultrasonic agitation for different durations of 3, 15, 30, and 45 min, which referred to as $M_3$-3, $M_3$-15, $M_3$-30, and $M_3$-45, respectively.

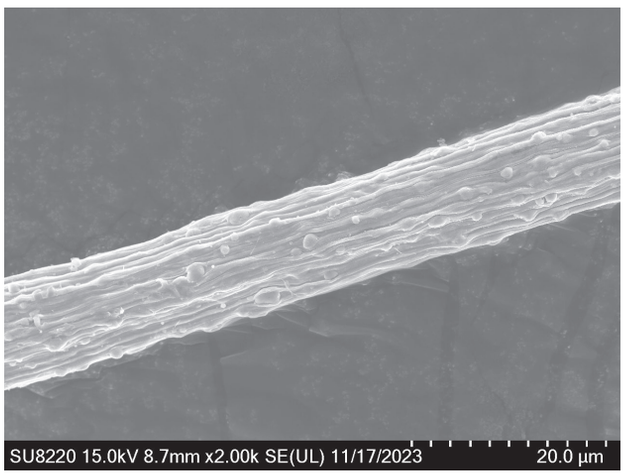


**Fig. 1: Microstructure of a single steel fiber**

**Table 1: Raw materials for preparation of steel-fiber-reinforced shell slurry**

| Slurry | Binder | Filler (mesh) | Binder: filler (g:g) | Stirring method | Stucco sand (mesh) | Drying time (h) |
|---|---|---|---|---|---|---|
| Primary layer (1) | Silica sol (25%) | Zircon sand (325) | 1:3.0 | Mechanical stirring for 24 h | Zircon sand (100–120) | 12 |
| Transition layer (2) | | Mullite sand (200) | 1:1.6 | Mechanical stirring for 12 h | Mullite sand (30–60) | 24 |
| Back layer (3, 4) | | Mullite sand (200) | 1:1.4 | Fiber: Steel fibers (0.15% of the weight of filler)<br>$M_1$ (traditional method)<br>$M_2$ (added fiber into silica sol with mechanical stirring and ultrasonic agitation)<br>$M_3$ (added fiber into slurry with mechanical stirring and ultrasonic agitation for 3, 15, 30, 45 min) | Mullite sand (16–30) | 24 |
| Sealing layer (5) | | | | | – | 24 |

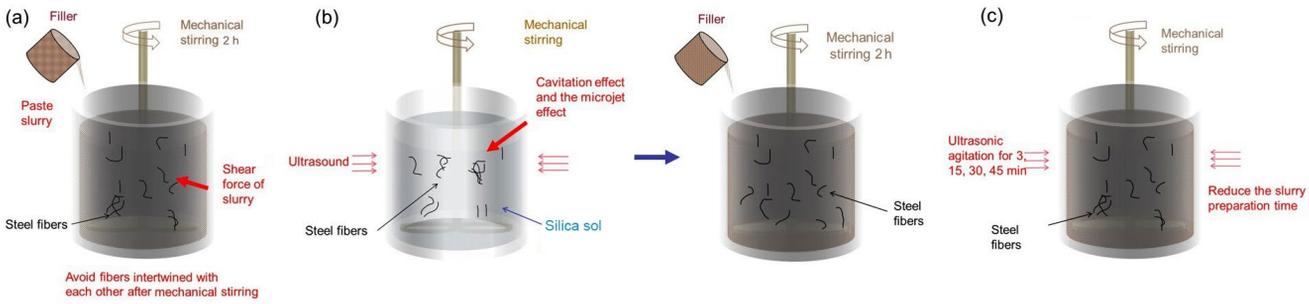


**Fig. 2: Slurry preparation methods: (a) $M_1$; (b) $M_2$; (c) $M_3$**

Notably, the durations of 15 min, 30 min, and 45 min correspond to the entire preparation time of the slurry, encompassing both mechanical stirring and ultrasonic agitation after the fiber and filler have been added to the silica sol. However, in the case of $M_3$-3, the slurry undergoes an initial 2 h period of mechanical stirring, followed by an additional 3 min of combined mechanical stirring and ultrasonic agitation.

After the slurry had been prepared, it was smeared onto the wax pattern, followed by the stuccoing of sand. Once the slurry had dried, the investment casting shell specimen was obtained through dewaxing. Subsequently, the specimens intended for high-temperature testing were fired according to the procedure illustrated in Fig. 3.

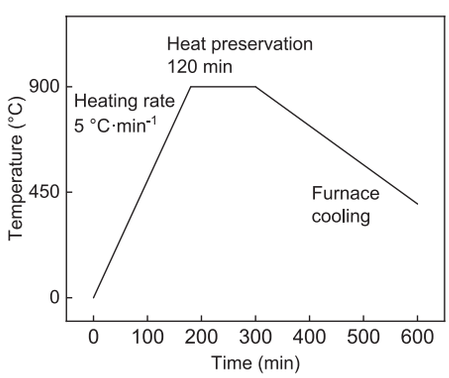


**Fig. 3: Firing process route**

## 2.2 Measurements

The bending strength specimen size was shown in Fig. 4(a). The bending strength testing of the shell molds is carried out on a tensile testing machine, type TKW (Xiangtan Xiangyi Instrument Co. Ltd., China), using the three-point bending test method, at a loading rate of 6 mm·min$^{-1}$, according to the HB5352.1-2004 China Aeronautical Standard. A scanning electron microscope (SEM, S-3400N) was used to observe the surface microstructure and the distribution of fiber in the shell.

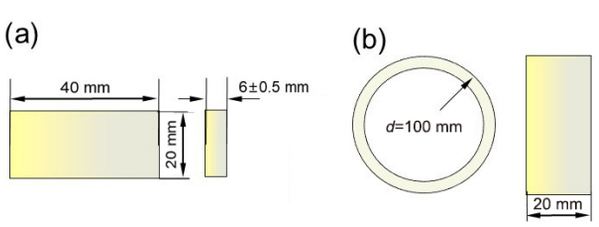


**Fig. 4: Specimen sizes: (a) bending strength specimen; (b) high-temperature self-load deformation specimen**

The high-temperature self-load deformation of the shell mold was determined according to the HB5352.2-2004 China Aeronautical Standard, and the specimen size is shown in Fig. 4(b). The fired specimens were heated to 1,200 °C at a rate of 10 °C·min$^{-1}$ and held for 1 h at this temperature. Once it was cooled down in the furnace, its deformation amount was measured.

The thermal conductivity of the specimens was assessed using a hot disk method (TPS3500s, Hot Disk, Sweden). The specimen size was the same as that in the bending strength testing. Before the measurements, the hot disk probe was placed in the middle of the same specimen. Once the current passed through the probe, a certain temperature rise was induced. The heat generated is diffused to the specimen from simultaneously both sides of the probe. By recording the temperature and response time of the probe, the thermal conductivity can be obtained directly from the mathematical model.

# 3 Results and discussion

## 3.1 Bending strength of fiber-reinforced shell molds

As shown in Fig. 5, the shell mold fabricated utilizing Method $M_2$ achieves the highest green bending strength of 3.29 MPa, which represents a 29% enhancement over the strength exhibited by the mold produced through the $M_1$ process. It can be concluded that the dispersion of steel fibers can effectively improve the shell strength. The distribution of fibers in the shell is depicted in Figs. 6(a–c). Without ultrasonic agitation [Fig. 6(a)], the fibers are intertwined with each other. While, in the shell prepared by the

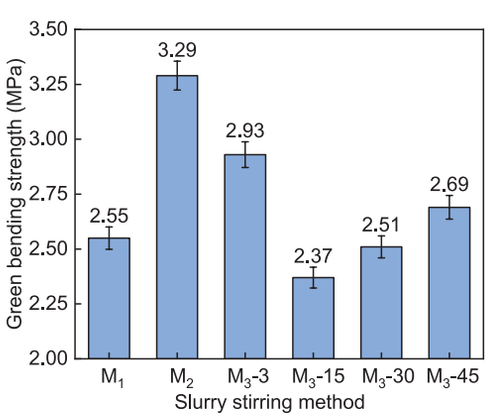


**Fig. 5: Green bending strength of shell molds prepared using different methods**

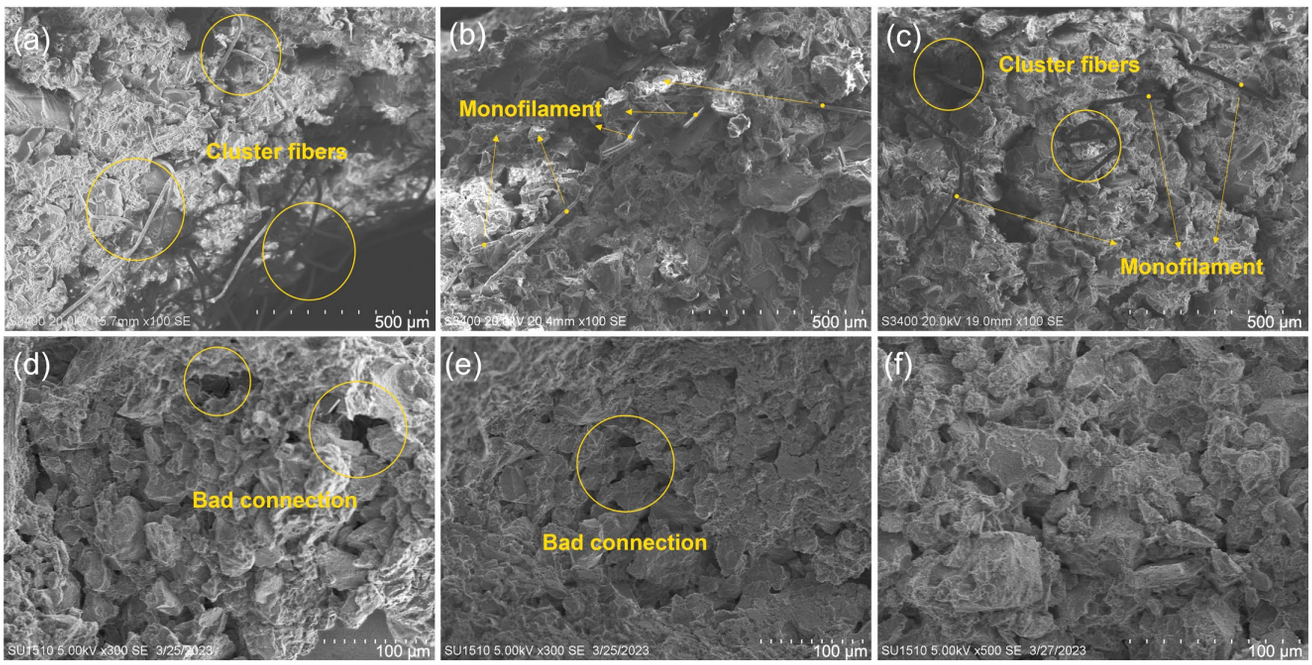


**Fig. 6: Micromorphology and fracture characteristics of shell molds prepared using different methods: (a) $M_1$; (b) $M_2$; (c) $M_3$-3; (d) $M_3$-15; (e) $M_3$-30; and (f) $M_3$-45**

$M_2$ method, the majority of the fibers exist in a monofilament state and are distributed in various random directions, forming a robust bond with the shell mold. The deformation and fracture of fibers, as well as the delamination and extraction between the fibers and shell, can effectively resist the fracture load during failure. Moreover, the purpose of preparing the slurry via the method $M_3$-3 is to reduce the negative impact of fiber entanglement during mechanical stirring. However, the strength is reduced by 11% compared with the shell mold prepared by $M_2$. As shown in Fig. 6(c), the dispersion of fibers is not realized in the shell prepared by $M_3$-3, and some fibers are still intertwined, compromising the strength of the shell mold.

As shown in Fig. 7(a), under the influence of ultrasonic, the force generated by the cavitation and microjet effects directly acts on the fibers. At this time, the van der Waals forces between fibers are destroyed and the state of motion balance is reached. Moreover, fibers are evenly dispersed in the silica sol with mechanical stirring. While, when adding fibers in slurry, as shown in Fig. 7(b), most of the forces are hindered by the fillers and only a small part acts on the fibers. Therefore, although the filler is dispersed, the fibers are easier to intertwine under the influence of mechanical stirring shear force and large surface friction of fibers. For the shell prepared by $M_3$-15, 30, and 45 (Fig. 5), the strength of the shell increases with the ultrasonic agitation time, but remains close to that of the shell prepared by $M_1$. As mentioned earlier, the forces generated by ultrasonication mostly act on the filler, impeding uniform dispersion of fibers in the silica sol due to the short ultrasonication time [Fig. 6(d)]. After the shell has dried, the silica sol undergoes gelation and does not form a secure attachment with certain sections of the filler. With the increase of ultrasonic agitation time, the filler is gradually dispersed in the silica sol, as shown in Figs. 6(e, f). As soon as the filler and silica sol are completely bonded, the strength of the shell is improved. Therefore, even though the fiber dispersion is improved to a small extent, the preparation time of the slurry is effectively reduced by using ultrasonication and mechanical stirring at the same time.

The fired bending strength of the shell mold is depicted in Fig. 8. After firing, the free water and constitution water in the shell mold are completely dried. The microstructure becomes dense and the fired strength is greatly improved compared to

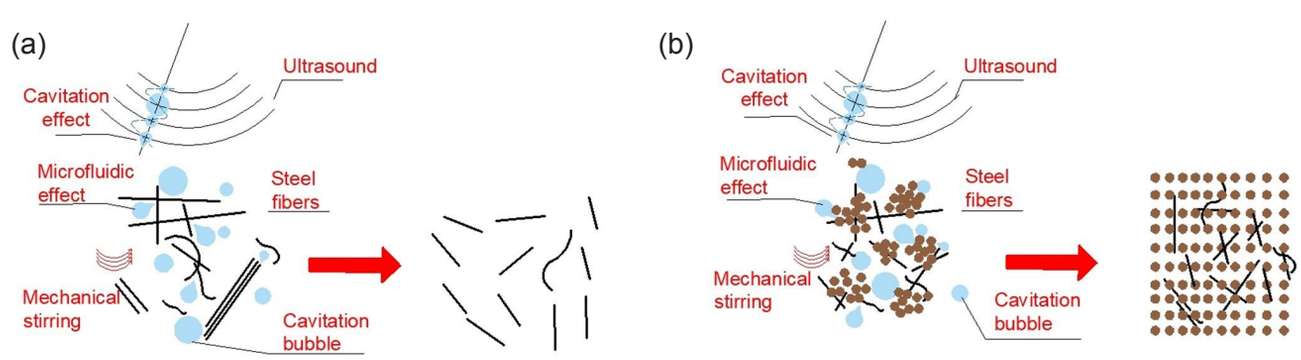


**Fig. 7: Effect of ultrasonication on fibers in silica sol (a) and slurry (b)**

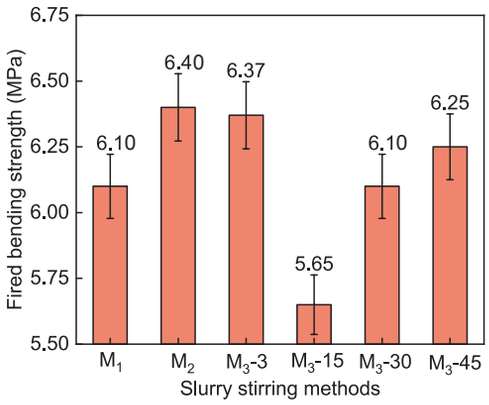


**Fig. 8: Fired bending strength of the shell mold by different methods**

the green bending strength. The highest fired bending strength of the shell mold is achieved via the method $M_2$ (6.40 MPa), being 4% higher than that of the shell mold prepared by the traditional method. As shown in Fig. 9(a), the monofilament is tightly bonded to the matrix and the fiber plays a certain role in hindering the crack growth or promoting the crack turning. Therefore, during the shell fracture, the fibers could effectively resist the partial fracture load and increase the bending strength of the shell. Figure 9(b) displays the intertwined fibers in the matrix. After firing, the filler expands, leading to a denser microstructure and smaller pores within the intertwined fibers. Compared to its bending strength before firing, the improved bonding between the fibers and the matrix ensures a certain level of resistance to fracture load during failure.

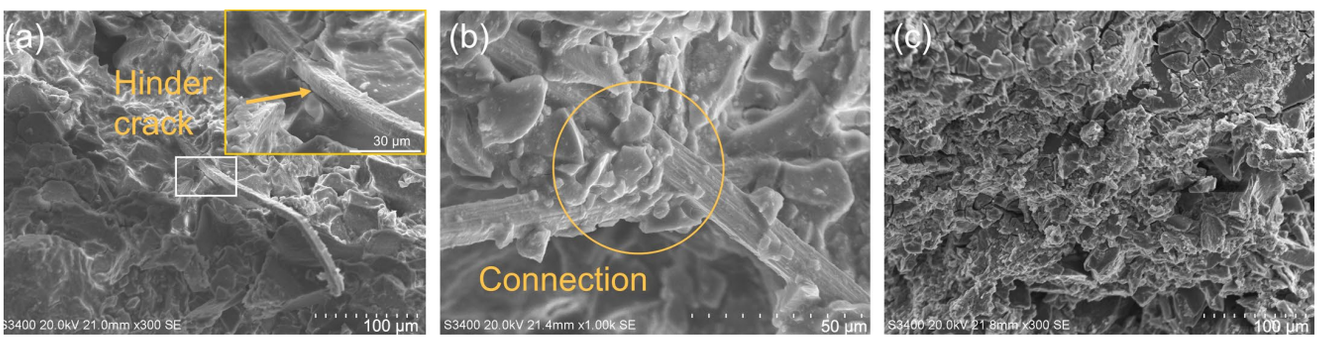


**Fig. 9: Micromorphology and fracture characteristics of the fired shell mold: (a) monofilament by $M_2$; (b) intertwined fibers by $M_3$-3; and (c) matrix of shell prepared by $M_3$-45**

The changing trend of fired bending strength of the shell mold prepared via $M_3$ is similar to the green bending strength, which is mainly affected by the uniformity of the filler. After the slurry is stirred, the adsorbed gas on the surface of the filler is removed. Hence, the filler is completely wet and evenly disperses in the silica sol. However, at a shorter stirring time of the slurry, the filler disperses unevenly, affecting the fluidity and coating performance of the slurry. Moreover, the filler exhibits the localized segregation. This negative effect on the shell mold is further amplified after firing because the binder and filler could not be completely sintered at high temperatures, thereby forming a crack source, which reduces the strength of the shell mold. At the ultrasonic agitation time of 15 min, the green strength is close to that attained in the traditional method. Meanwhile, the strength after firing is 7% lower than that of the traditionally prepared specimen. This is because, with an increase in ultrasonic agitation time, the filler could be evenly dispersed in a short time. After the ultrasonic agitation for 45 min, the refractory powder is uniformly dispersed in the silica sol and the dispersion effect is consistent with that of the mechanical stirring for 2 h in $M_1$, as shown in Fig. 9(c). After firing, a good skeleton structure is formed, and the strength reaches 6.25 MPa. Therefore, the shell mold prepared by $M_3$-45 can meet the application requirements.

## 3.2 High-temperature self-load deformation of fiber-reinforced shell molds

Figure 10 shows the high-temperature self-load deformation of the shell. The dispersion of fibers in the shell significantly

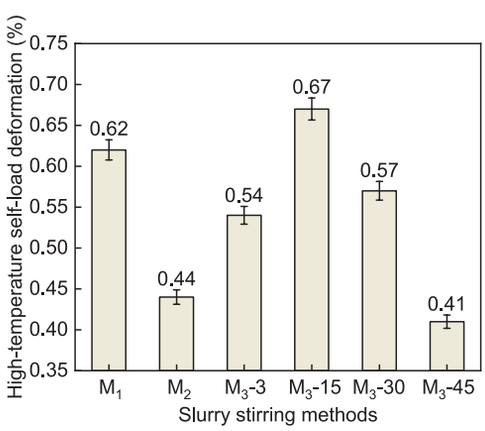


**Fig. 10: High-temperature self-load deformation of shell molds prepared using different methods**

affects the deformation behavior of the shell mold. For the shell mold prepared via the Method $M_3$-45, the minimum high temperature self-load deformation is 0.41%. Similarly, for the well dispersed fibers ($M_2$ method), the monofilaments form a mesh structure in the shell mold, which act as a reinforcement and prevent shell deformation, thus a small high-temperature self-load deformation is obtained. On the contrary, when the shell mold is prepared by $M_1$, the high-temperature self-load deformation is great, the fibers are intertwined with each other, which deteriorates the brace effect and increases the deformation. With the same firing temperature, the dispersion uniformity of the filler is the main factor affecting the high temperature self-load deformation of the shell mold

prepared by $M_3$-15, 30, and 45. When the ultrasonic agitation time is 15 min, the filler is not uniformly dispersed within the slurry. The mesh skeleton could not be formed and the brace effect on the shell is weak. On the contrary, after 45 min, the filler is completely dispersed and the high-temperature self-load deformation reaches the minimal level.

### 3.3 Heat conduction of fiber-reinforced shell molds

Figure 11 depicts the thermal conductivity of shell molds prepared by different methods. For the shell mold produced via the $M_1$ method, the fibers intertwine with each other, resulting in a low thermal conductivity. For the shell molds obtained via the $M_2$ and $M_3$-3 methods, the thermal conductivity is high, this is because the fiber dispersion is improved and the monofilament in the shell could quickly transfer the heat to the outer wall of the shell mold. The different thermal conductivity of the shell mold prepared by $M_3$-15, 30, and 45 methods is not due to the dispersion of the fibers; instead, the thermal conductivity is mainly affected by the uniformity of the filler. With a short ultrasonic agitation time, the porosity of the shell mold increases due to the presence of the unevenly distributed filler. This changes the heat transfer mode from conduction to radiation, consequently reducing the thermal conductivity. Furthermore, the thermal conductivity of the shell mold is improved with the increase of ultrasonic agitation time. Nevertheless, the overall thermal conductivity remains low because the enhancement in fiber dispersion is minimal.

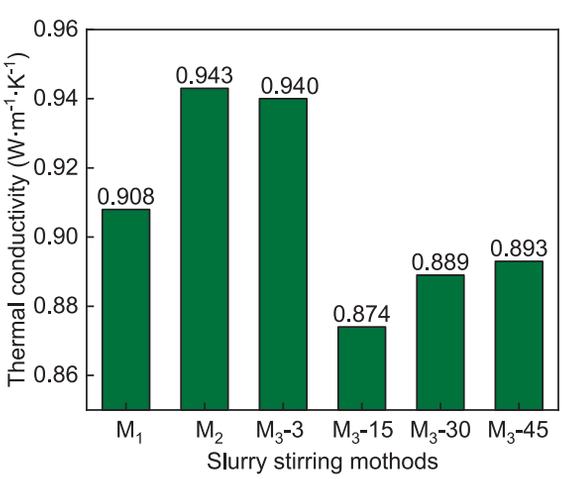


**Fig. 11: Thermal conductivity of shell molds prepared by different methods**

In the steel-fiber reinforced shell mold, the thermal conductivity of the steel fiber is 16.3 $W·m^{-1}·K^{-1}$, while the thermal conductivity of the shell matrix is only 0.87 $W·m^{-1}·K^{-1}$. Under the same temperature gradient, heat is preferentially transferred along the fibers, enhancing the thermal conduction of the shell. Due to the influence of slurry and stucco sands, the fibers are distributed within the shell mold in a disorderly manner. Consequently, heat transfer manner is affected by this fiber distribution. As shown in Fig. 12(a), after passing through the primary and transition layers, the heat encounters the back layer. There are two different modes of heat transfer: One is through the fibers, and the other is through the matrix. The heat is preferentially transferred along the fibers. However, if the fiber is deformed, heat can only be transferred in the direction of decreasing temperature (i.e., through the matrix). When the heat passes through the matrix and meets the fiber, it continues to transfer along the fiber, improving the overall heat conductivity of the shell. When the axial direction of the fiber is perpendicular to the direction of heat transfer, as shown in Fig. 12(b), the fiber exerts the most pronounced strengthening effect on the shell mold. However, when the heat passes through the fibers, this strengthening effect becomes negligible. The optimal distribution of fibers in the shell mold is shown in Fig. 12(c). The fibers exist in the interstice of the stucco sands and spread through the three layers. When the heat passes through the fiber, it can be quickly transferred to the outer wall of the shell mold[21, 22]. The reinforcement effect gets worse when the fibers are clustered together. This clustering not only fails to enhance the strength of the shell mold but also slows down the heat transfer process, as shown in Fig. 12(d), the heat continues to pass through the matrix and fiber, slowing the transfer speed and even leading to heat accumulation around the clustered fibers. In addition, if the pores within the clustered fibers change the mode of heat transfer from conduction to radiation, the thermal conductivity is further compromised.

Meanwhile, in order to invesigate the changes in thermal conductivity of the shell mold during pouring, a self-designed pouring device was used. The measurements were taken in the radial direction of heat transfer in cylindrical castings, and the axial direction of heat transfer was ignored. The dimensions and shapes of the specimen are illustrated in Fig. 13. Before the shell mold preparation, the ceramic tube was placed at the center of the wax pattern, inner and outer walls of the shell mold. Then, after dewaxing and firing, the thermocouple was installed in ceramic tubes to record the cooling

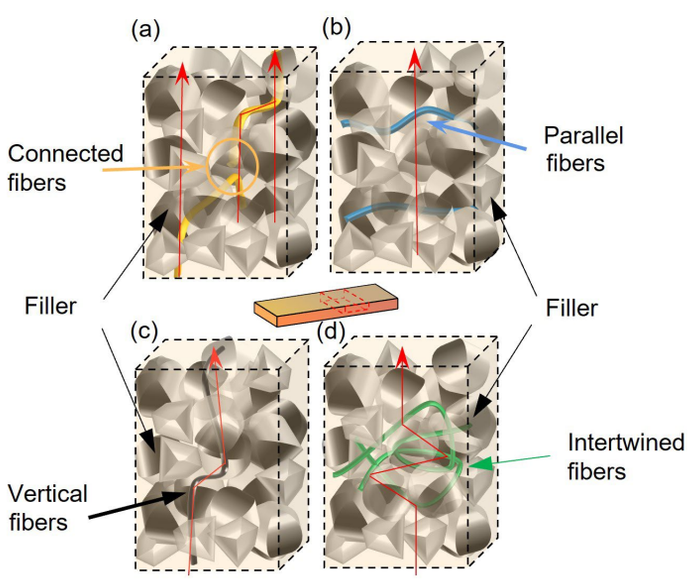


**Fig. 12: Heat transfer in the shell: (a) connected fibers; (b) parallel fibers; (c) vertical fibers; (d) intertwined fibers**

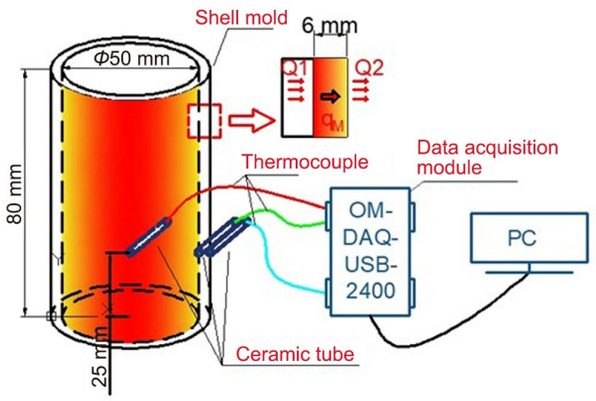


**Fig. 13: Test device diagram showing thermal conductivity measurement of the shell mold**

curve at each point after pouring. Since the same metal was used for pouring, the pouring temperature and external environment remained the same and the heat flux through the shell mold was kept unchanged. In addition, the greater the thermal conductivity of the shell mold, the smaller the temperature gradient between the inner and outer walls of the shell mold. This results in the temperature curves of the inner and outer walls of the shell mold being closer. Conversely, a smaller thermal conductivity leads to a larger temperature gradient and more divergent temperature curves between the inner and outer walls. This can be expressed as follows:

$$q_M = \frac{\Delta Q_M}{\Delta A} = -\lambda \frac{dT}{dx} \quad (1)$$

where $q_M$ is heat flux across the shell mold ($W \cdot m^{-2}$); $A$ refers to the area of thermal conduction ($m^2$); $Q_M$ is the heat transferred across the shell mold (W); $\lambda$ represents the thermal conductivity ($W \cdot m^{-1} \cdot K^{-1}$); and $\frac{dT}{dx}$ stands for the temperature gradient ($K \cdot m^{-1}$).

Figure 14 displays the cooling curves of the shell mold prepared by different methods after pouring. The thermal conductivity of different shell molds can be determined by comparing the closeness of the temperature curves between the inner and outer walls. However, the closeness cannot be directly assessed. Hence, a root mean square error (RSME) is introduced[23, 24], which is a statistical concept used to evaluate the closeness between the observed and real values as follows:

$$RMSE = \sqrt{\frac{1}{n}\sum_{i=1}^{n}(T_{inner} - T_{outer})^2} \quad (2)$$

where $n$ refers to the number of samples. The smaller RMSE corresponds to the closer curves and the better thermal conductivity.

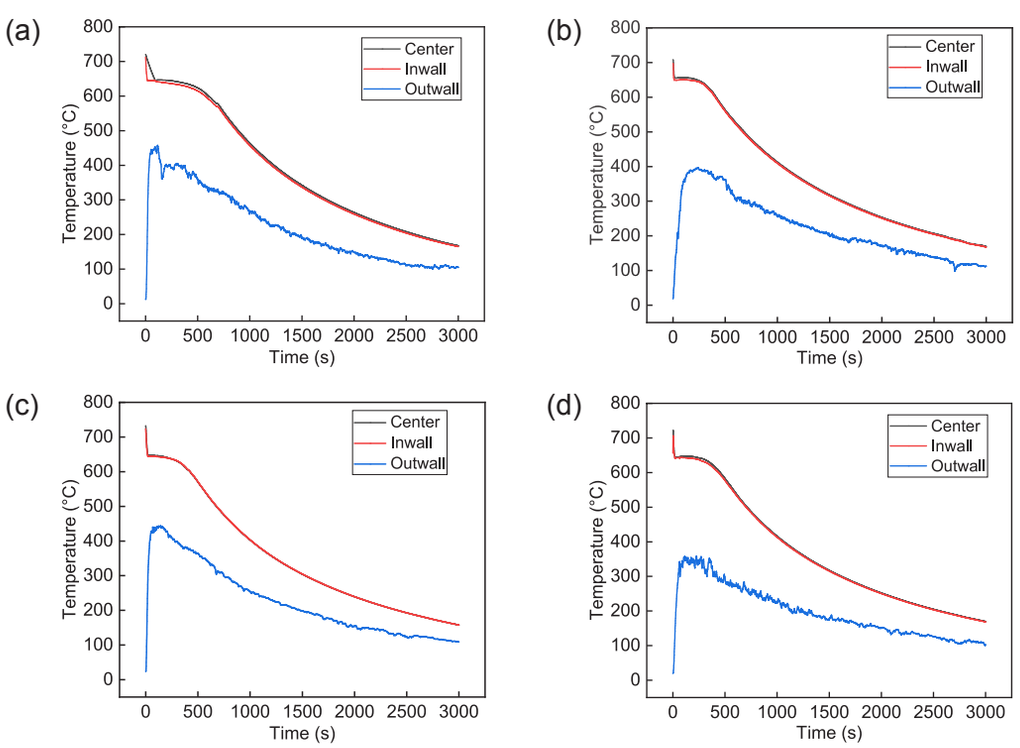


**Fig. 14: Temperature variation of the shell molds prepared using different methods: (a) $M_1$; (b) $M_2$; (c) $M_3$-3; (d) $M_3$-45**

**Table 2: Temperature analysis of shell molds prepared by different methods**

| Slurry stirring methods | $M_1$ | $M_2$ | $M_3$-3 | $M_3$-45 |
|---|---|---|---|---|
| RMSE | 181.92 | 90.84 | 144.36 | 185.48 |

The calculated RMSE values are given in Table 2. The smallest RMSE is obtained when the shell mold is prepared by $M_2$. Hence, the closest curve and the best thermal conduction can be ensured. Therefore, improving the dispersion of steel fiber within the shell mold can enhance the thermal conductivity of the shell mold.

## 4 Conclusions

To improve the dispersion of steel fibers in the shell mold, two different ultrasonic agitation techniques were designed that one is adding fibers to silica sol and the other is to slurry. These two methods were compared with the traditional method. The green bending strength, fired bending strength, high-temperature self-load deformation, and thermal conductivity of the shell molds prepared by different methods were investigated in detail. Based on the findings, the following conclusions can be drawn:

(1) When ultrasonic agitation is used to disperse the fibers in silica sol in combination with mechanical stirring, the fiber dispersion in the shell mold can be improved effectively, which enhances the strength of the shell mold. The maximum green bending strength is found to be 3.29 MPa, which is 29% higher than that of the shell mold prepared by the traditional method. The high temperature self-load deformation is found to be 0.44%, and the same shell mold also exhibits the optimal thermal conductivity of 0.943 $W \cdot m^{-1} \cdot K^{-1}$.

(2) When using the method that adding fibers to slurry, ultrasonic agitation cannot effectively disperse the fibers due to the presence of fillers. Therefore, this method is not conducive to the preparation of shells.

(3) Simultaneous use of ultrasonic agitation and mechanical stirring can effectively shorten the preparation time of the slurry. When the slurry preparation time is reduced to 45 min, the fired bending strength can reach up to 6.25 MPa, and the high-temperature self-load deformation is found to be 0.41%. Thus, the performance can achieve the level of the shell mold produced via the conventional method.

## Acknowledgments

This work was supported by the National Natural Science Foundation of China (Grant No. 5186504), the University Science Foundation for Young Science and Technology Talents in Inner Mongolia Autonomous Region of China (Grant No. NJYT22078), the Basic Scientific Research Expenses Program of Universities directly under Inner Mongolia Autonomous Region (Grant No. JY20220059), the Inner Mongolia Autonomous Region 'Grassland Talent' project Young Innovative Talent Training Program Level I, and Basic Research Expenses of Universities directly under the Inner Mongolia Autonomous Region (Grant No. ZTY2023040).

## Conflict of interest

The authors declare that this work is original and has not been previously published elsewhere, nor is it currently under consideration for publication elsewhere. All authors listed have endorsed the manuscript as submitted. There are no conflicts of interest associated with the submission of this manuscript, and all authors have approved the manuscript for publication.

## References

[1] Pattnaik S, Karunakar D B, Jha P K. Developments in investment casting process – A review. Journal of Materials Processing Technology, 2012, 212(11): 2332–2348. https://doi.org/10.1016/j.jmatprotec.2012.06.003

[2] Wei Y M, Lü Z G, Guo X. Influence of alkaline oxide on the deformation of ceramic shell mould at high temperatures during investment casting. Ceramics International, 2018, 44(17): 21197–21204. https://doi.org/10.1016/j.ceramint.2018.08.165

[3] Kumar S, Karunakar D B. Enhancing the permeability and properties of ceramic shell in investment casting process using ABS powder and needle coke. International Journal of Metalcasting, 2019, 13: 588–596. https://doi.org/10.1007/s40962-018-00297-7

[4] Venkat Y, Choudary K R, Chatterjee D, et al. Development of mullite-alumina ceramic shells for precision investment casting of single-crystal high-pressure turbine blades. Ceramics International, 2022, 48(19): 28199–28106. https://doi.org/10.1016/j.ceramint.2022.06.124

[5] Znamenskii L G, Ivochkina O V, Varlamov A S. Acceleration of the formation on the sodium silicate binder in investment casting. Materials Science Forum, 2019, 4726(94): 673–677. https://doi.org/10.4028/www.scientific.net/MSF.946.673

[6] Harun Z, Kamarudin N H, Ibrahim M, et al. Reinforced green ceramic shell mould for investment casting process. Advanced Materials Research, 2015, 1087: 415–419. https://doi.org/10.4028/www.scientific.net/AMR.1087.415

[7] Li Z X, Liu X D, Lu Y, et al. Influence of rice husk on the properties of fiber-reinforced silicon sol shells used in investment casting process. Journal of Adhesion Science and Technology, 2021, 36(5): 469–489. https://doi.org/10.1080/01694243.2021.1926826

[8] Raza M, Irwin M, Fagerström B. The effect of shell thickness, insulation and casting temperature on defects formation during investment casting of Ni-base turbine blades. Archives of Foundry Engineering, 2015, 15(4): 115–123. https://doi.org/10.1515/afe-2015-0090

[9] Xiao Z Y, Dong S Q, Nie S, et al. Simulation of the solidification organization of X15CrNiSi20-12 alloy castings during investment casting based on the CAFE model. Journal of Physics: Conference Series, 2023, 2419(1): 012075.

[10] Yuan C, Jones S. Investigation of fiber modified ceramic molds for investment casting. Journal of the European Ceramic Society, 2003, 23: 399–407. https://doi.org/10.1016/633S0955-2219(02)00153-X

[11] Li Y F, Liu X D, Lü K, et al. Exploration on preparation process of high-strength fiber-reinforced shell for investment casting. International Journal of Metalcasting, 2021, 15: 692–699

[12] Lü K, Liu X D, Duan Z H. Effect of firing temperature and time on hybrid fiber-reinforced shell for investment casting. International Journal of Metalcasting, 2019, 13: 666–673. https://doi.org/10.1007/s40962-018-0280-x

[13] Lü K, Shen S M, Ma C Q, et al. Research on modification of steel fiber in investment casting shell. International Journal of Metalcasting, 2022, 16: 1849–1857. https://doi.org/10.1007/s40962-021-00722-4

[14] Ren J, Chen X, Li Y X, et al. Properties of fiber reinforced plaster molds for investment casting. China Foundry, 2020, 17(4): 332–340. https://doi.org/10.1007/s41230-020-0056-9

[15] Lu G, Chen Y, Yan Q, et al. Carbon-nylon hybrid fibers modified silica sol shell with enhanced flexural strength and heat transfer for investment casting. Journal of the European Ceramic Society, 2022, 42(8): 3624–3633. https://doi.org/10.1016/j.jeurceramsoc.2022.03.010

[16] Lü K, Duan Z H, Liu X D, et al. Effects of fibre length and mixing routes on fibre reinforced shell for investment casting. Ceramics International, 2019, 45(6): 6925–6930. https://doi.org/10.1016/j.ceramint.2018.12.189

[17] Pattnaik S, Sutar K M. Enhancement of ceramic slurry rheology in investment casting process. Arabian Journal for Science and Engineering, 2021, 46(12): 1–12. https://doi.org/10.1007/s13369-021-05834-x

[18] Wang S M, Zou Q L, Zhang L W. A new nanocellulose prepared from waste coconut shell fibers based on a novel ultrasonic-active agent combination method: Preparation principle and performances in cement matrix. Industrial Crops and Products, 2023, 197: 116607. https://doi.org/10.1016/j.indcrop.2023.116607

[19] Ci M, Liu J, Liu L. Preparation and characterization of hydroxypropyl methylcellulose modified alginate fiber. Journal of Physics: Conference Series, 2021, 1790: 012073. https://doi.org/10.1088/1742-6596/1790/1/012073

[20] Kumar A, Nirala A, Singh V P. The utilisation of coconut shell ash in production of hybrid composite: Microstructural characterisation and performance analysis. Journal of Cleaner Production, 2023, 398: 136494. https://doi.org/10.1016/j.jclepro.2023.136494

[21] Fang Z N, Li M, Wang S K, et al. Geometrical effect on thermal conductivity of unidirectional fiber-reinforced polymer composite along different in-plane orientations. Applied Thermal Engineering, 2018, 25: 1255–1268. https://doi.org/10.1007/s10443-017-9664-y

[22] Ren Q L, Wang Z X, Lai T, et al. Conjugate heat transfer in anisotropic woven metal fiberphase change material composite. Applied Thermal Engineering, 2021, 189: 116618. https://doi.org/10.1016/j.applthermaleng

[23] Faria A J G, Silva S H G, Melo L C A, et al. Soils of the Brazilian coastal plains biome: Prediction of chemical attributes via portable X-ray fluorescence (pXRF) spectrometry and robust prediction models. Soil Research, 2020, 58: 683–695.

[24] Li J, Wang C X, Yue L, et al. Nano-QSAR modeling for predicting the cytotoxicity of metallic and metal oxide nanoparticles: A review. Ecotoxicology and Environmental Safety, 2022, 243: 113955. https://doi.org/10.669 1016/j.ecoenv.2022.113955